MULTI-SOURCE COOPERATION WITH FULL-DIVERSITY SPECTRAL-EFFICIENCY AND CONTROLLABLE-COMPLEXITY

Alejandro Ribeiro, Renqiu Wang and Georgios B. Giannakis

Dept. of ECE, University of Minnesota, 200 Union Street, Minneapolis, MN 55455, USA

ABSTRACT

We develop a general framework for multi-source cooperation (MSC) protocols to improve diversity and spectral efficiency relative to repetition based alternatives that rely on single-source cooperation. The novel protocols are flexible to balance tradeoffs among diversity, spectral efficiency and decoding-complexity. Users are grouped in clusters and follow a two-phase MSC protocol which involves time division multiple access (TDMA) to separate users within a cluster, and code division multiple access (CDMA) to separate clusters. An attractive protocol under the general MSC framework, relies on distributed complex field coding (DCFC) to enable diversity order equal to the number of users per cluster. Cluster separation based on orthonormal spreading sequences leads to spectral efficiency $1/2$. When the number of clusters exceeds the amount of spreading, spectral efficiency can be enhanced without sacrificing diversity, at the expense of controllable increase in complexity.

1. INTRODUCTION

Cooperative diversity is a recently introduced fading countermeasure in which single-antenna terminals cooperate to effect a virtual distributed antenna array. Early cooperative approaches were mainly based on distributed repetition coding, according to which cooperating users repeat or re-encode the information bearing message received from a single source to the destination by either amplifying-and-forwarding or regenerating operations [3, 4]. Unfortunately, the resultant increase in diversity comes at the price of spectral efficiency loss – that can be mitigated with the use of distributed space-time codes [1]. Multi-source cooperation (MSC), relying on joint coding of multiple sources was introduced in [5] to improve bandwidth efficiency and diversity order. Building on these results, two-phase MSC systems with distributed convolutional coding and distributed trellis coded modulation were reported in e.g., [2, 6]. With $d_{\min}$ and R_c denote respectively the minimum (free) distance and the rate of an error control code (ECC), the maximum achievable diversity order effected by ECC in MSC networks with K users is $\eta = \min(d_{\min}, \lfloor 1 + K(1 - R_c)\rfloor)$ – falling short of the maximum available diversity K.

* Work in this paper was prepared through collaborative participation in the Communications and Networks Consortium sponsored by the U. S. Army Research Laboratory under the Collaborative Technology Alliance Program, Cooperative Agreement DAAD19-01-2-0011. The U. S. Government is authorized to reproduce and distribute reprints for Government purposes notwithstanding any copyright notation thereon The views and conclusions contained in this document are those of the authors and should not be interpreted as representing the official policies, either expressed or implied, of the Army Research Laboratory or the U. S. Government..

This paper introduces a general MSC framework with full-diversity, flexible spectral efficiency and controllable decoding complexity. Users are grouped in clusters that are separated with code division multiple access (CDMA). Within each cluster users cooperate to reach the access point (AP), implementing MSC according to a two-phase TDMA protocol (Section 2). The first contribution of the present work is to show that the diversity order of a general MSC protocol coincides with the diversity order when the links between cooperating users are error-free (Section 2.1). As the latter can be thought as a single user transmission over single input - multiple output (SIMO) channels, two implications of this result are: i) the diversity order of repetition coding is $\eta_{\mathrm{RC}} = 2$; and ii) the maximum diversity order of distributed ECC is $\eta_{\mathrm{DECC}} = \min(d_{\min}, \lfloor 1 + K(1 - R_c)\rfloor)$. The second contribution of this paper is to establish that CFC-based MSC enables diversity order equal to the number of users, $\eta_{\mathrm{CFC}} = K$ (Section 2.2). We further address cluster separation and demonstrate that when the number of clusters is larger than the spreading gain, flexible MSC protocols emerge trading off spectral efficiency, error performance and complexity (Section 3). While coding gain is affected by the use of non-orthonormal spreading the diversity order is not, thus enabling MSC protocols to achieve full diversity at maximum spectral-efficiency equal to that of non-cooperative networks (Section 4).

2. MULTI-SOURCE COOPERATION

Consider a cooperative multiple access (MA) setup in which the set of active users is divided into L clusters $\{\mathcal{U}_l\}_{l=1}^{L}$. Within each cluster, K_l users $\{U_{lk}\}_{k=1}^{K_l}$ cooperate in transmitting symbol blocks $\mathbf{s}_{lk} := [s_{lk1}, \ldots, s_{lkN}]^T$ of size $N \times 1$ to the AP (U_{00}). We assume that $\mathbf{s}_{lk}$ contains a cyclic redundancy check (CRC) code to screen incorrectly received packets. We let $\mathbf{h}_{l_1k_1,l_2k_2} := h_{l_1k_1,l_2k_2}\mathbf{1}_N$ denote the block Rayleigh fading channel between users $U_{l_1k_1}$ and $U_{l_2k_2}$; and $\mathbf{h}_{lk} := h_{lk}\mathbf{1}_N$ the one between U_{lk} and the AP. We further assume that these channels are uncorrelated. Let us focus on the operation of a single cluster, for which we set $L = 1$ and drop the cluster subscript l to simplify notation.

Supposing that frame synchronization has been established, TDMA is used to separate users per cluster as depicted in Fig. 1. The MSC protocol consists of two phases each taking place over K slots. Upon defining the aggregate $KN \times 1$ transmitted and received blocks $\mathbf{s} := [\mathbf{s}_1^T, \ldots, \mathbf{s}_K^T]^T$ and $\mathbf{y}_k^{(1)} := [y_{k,11}, \ldots, y_{k,1N}, y_{k,21}, \ldots, y_{k,KN}]^T$, the AWGN $\mathbf{n}_k^{(1)} := [n_{k,11}, \ldots, n_{k,KN}]^T$ and the diagonal channel matrix $\mathbf{D}_k^{(1)} := \mathrm{diag}(\mathbf{h}_{k,1}^T, \ldots, \mathbf{h}_{k,N}^T)$, the input-output relationship per user U_k during phase-1 is

$$\mathbf{y}_k^{(1)} = A\mathbf{D}_k^{(1)}\mathbf{s} + \mathbf{n}_k^{(1)}, \qquad k = 0, 1, \ldots, K, \quad (1)$$

where by convention $\mathbf{h}_{k,k} \equiv \mathbf{1}_N \; \forall k$, $n_{k,kn} \equiv 0$ for $n \in [1, N]$

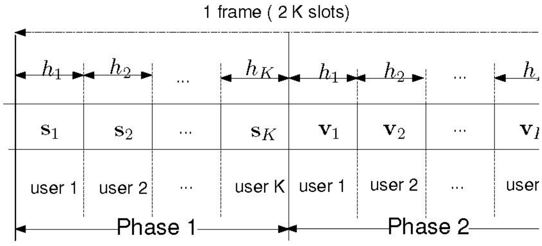

Fig. 1. Two-phase MSC for a cluster with K act

and we recall that $\mathbf{y}_0^{(1)}$ corresponds to the receivec AP. For future use, we note that the transmit SNR is

Notice that by the end of phase-1 every user information about the symbol blocks of all users $\mathcal{U}$. User U_k $(k > 0)$ estimates the joint block $\mathbf{s}$, drawn from a signal constellation $\mathcal{S}$, using the ma hood (ML) decoder [c.f. (1)]

$$\hat{\mathbf{s}}_k = \arg \min_{\mathbf{s} \in \mathcal{S}^N} \|\mathbf{y}_k^{(1)} - A\mathbf{D}_k^{(1)}\mathbf{s}\|.$$

Since not all users in $\mathcal{U}$ decode $\mathbf{s}$ correctly, we def those that do as

$$\mathcal{D} := \{U_k \mid \hat{\mathbf{s}}_k = \mathbf{s}\} \subseteq \mathcal{U}. \tag{3}$$

Users in $\mathcal{D}$ proceed to phase-2, but before transmission they process $\mathbf{s}$ as shown in Fig. 2. The aggregate block $\mathbf{s}$ is fed to the interleaver Π_1, yielding $\mathbf{r} = \mathbf{\Pi}_1\mathbf{s}$. The interleaved block $\mathbf{r}$ is then encoded with a function $\psi(\cdot)$ to obtain $\mathbf{u} = \psi(\mathbf{r})$, which is subsequently fed to a second interleaver Π_2, to obtain the block $\mathbf{v} = \mathbf{\Pi}_2\mathbf{u}$. This processing per user in $\mathcal{D}$ can be summarized as

$$\mathbf{v} = \mathbf{\Pi}_2\mathbf{u} = \mathbf{\Pi}_2\psi(\mathbf{r}) = \mathbf{\Pi}_2\psi(\mathbf{\Pi}_1\mathbf{s}). \tag{4}$$

Since all operations in (4) preserve dimensionality, we have that the blocks $\mathbf{v}, \mathbf{u}, \mathbf{r} \in \mathbb{C}^{NK\times 1}$, the matrices $\mathbf{\Pi}_1, \mathbf{\Pi}_2 \in \mathbb{C}^{NK\times NK}$ and the encoder $\psi : \mathbb{C}^{NK\times 1} \to \mathbb{C}^{NK\times 1}$.

Each user in $\mathcal{D}$ transmits again in a TDMA fashion an $N \times 1$ sub-block of the block $\mathbf{v} := [v_{11}, \ldots, v_{1N}, v_{21}, \ldots, v_{KN}]^T$, with U_k transmitting the sub-block $\mathbf{v}_k := [v_{k1}, \ldots, v_{kN}]^T$. The AP receives $\mathbf{v}_k$ from all users $U_k \in \mathcal{D}$ and nothing from the remaining users $U_k \notin \mathcal{D}$. To describe this reception, define the $N \times 1$ channel vector $\mathbf{h}_k^{(2)} := \mathbf{h}_k$, if $U_k \in \mathcal{D}$; and $\mathbf{h}_k^{(2)} := \mathbf{0}_N$, otherwise; so that the received block at the AP in phase-2 is

$$\mathbf{y}_0^{(2)} = A\mathbf{D}_0^{(2)}\mathbf{\Pi}_2\psi(\mathbf{\Pi}_1\mathbf{s}) + \mathbf{n}_0^{(2)}, \tag{5}$$

where $\mathbf{D}_0^{(2)} := \mathrm{diag}(\mathbf{h}_1^{(2)}, \ldots, \mathbf{h}_K^{(2)})$. The blocks $\mathbf{y}_0^{(1)}$ and $\mathbf{y}_0^{(2)}$ received in the two phases can be combined to yield

$$\begin{bmatrix} \mathbf{y}_0^{(1)} \\ \mathbf{y}_0^{(2)} \end{bmatrix}_{2KN\times 1} = A \begin{bmatrix} \mathbf{D}_0^{(1)}\mathbf{s} \\ \mathbf{D}_0^{(2)}\mathbf{\Pi}_2\psi(\mathbf{\Pi}_1\mathbf{s}) \end{bmatrix} + \begin{bmatrix} \mathbf{n}_0^{(1)} \\ \mathbf{n}_0^{(2)} \end{bmatrix} \tag{6}$$

that the AP relies on to jointly decode $\mathbf{s}$. Note that all channels are assumed invariant over the duration of the two phases. Furthermore, since we transmit KN symbols in $2KN$ time slots, the spectral efficiency of single-cluster MSC is $\xi = 1/2$.

Defining a particular MSC protocol amounts to specifying the triplet $(\mathbf{\Pi}_2, \psi(\cdot), \mathbf{\Pi}_1)$ in (4). The diversity enabled by any MSC protocol is mainly determined by the encoder $\psi(\cdot)$; while the interleavers $\mathbf{\Pi}_1$ and $\mathbf{\Pi}_2$ distribute relayed symbols to different channels in order to effect the diversity order enabled by

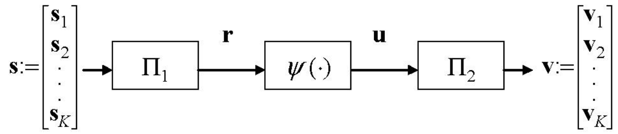

Fig. 2. Encoder and interleaver at each cooperating user.

$\psi(\cdot)$. Thus, the framework presented in this section subsumes a number of existing cooperative protocols as special cases:

[C1] Distributed repetition coding: Setting the permutation matrices $\mathbf{\Pi}_1 = \mathbf{\Pi}_2 = \mathbf{I}$ and selecting the encoder as

$$\psi_R(\mathbf{r}) = \psi_R(\mathbf{s}) = \psi_R([\mathbf{s}_1^T, \ldots, \mathbf{s}_K^T]^T) := [\mathbf{s}_2^T, \ldots, \mathbf{s}_K^T, \mathbf{s}_1^T]^T, \tag{7}$$

reduces input-output relations (1)-(5) to those encountered with MSC based on repetition coding whereby U_k repeats U_{k-1}'s frame for $k \neq 1$ and U_1 repeats U_K's frame, [4].

[C2] Distributed ECC: Let $\varphi(\cdot)$ be the function mapping a symbol vector over the *Galois field* $GF(m)$, to a channel codeword and $\varphi^{-1}(\cdot)$ the corresponding de-mapping function. Let also $\mathbf{P}$ denote the generator matrix of a channel encoder $\psi_P(\mathbf{r}) := \varphi(\mathbf{P}\varphi^{-1}(\mathbf{r}))$ with multiplication defined over $GF(m)$. If $\mathbf{P}$ generates a Reed-Solomon code, $\psi_P(\mathbf{r})$ specifies the MSC protocol in [5]; whereas if $\mathbf{P}$ generates a convolutional code, $\psi_P(\mathbf{r})$ gives rise to the DCC based MSC protocol in [2]. To effect the diversity, $\mathbf{\Pi}_1$ and $\mathbf{\Pi}_2$ have to be tailored for each chosen ECC [2]. Other channel codes, including distributed trellis coded modulation [6], are also possible choices.

[C3] Distributed CFC: Consider now the encoder $\psi_\Phi(\mathbf{r}) = \mathbf{\Phi}\mathbf{r}$, where $\mathbf{\Phi}$ is has complex entries and multiplication is over the *complex field*. This encoder $\psi(\cdot)$ amounts to distributed complex field coding (DCFC) that we will later elaborate on.

Remark 1 The encoder steps in (4) do not depend on $\mathcal{D}$, and consequently, the set $\mathcal{D}$ of users that correctly decoded $\mathbf{s}$ does not need to be known to the cooperating users.

2.1. Diversity Analysis

If $\mathbf{D}_0^{(1)}$ and $\mathbf{D}_0^{(2)}$ were Rayleigh distributed, (6) could model an $1 \times K$ SIMO channel with K receive antennas, or, a single antenna time-selective block fading channel with K degrees of freedom. In any event, the diversity order can be evaluated once the encoder $\psi(\cdot)$ has been specified. Alas, $\mathbf{D}_0^{(1)}$ is Rayleigh distributed but $\mathbf{D}_0^{(2)}$ is not. We will prove in this section that even if $\mathbf{D}_0^{(2)}$ is not Rayleigh distributed the diversity order of MSC coincides with the diversity order when $\mathbf{D}_0^{(2)}$ is Rayleigh distributed.

When the links between cooperating users are error-free $\mathcal{D} \equiv \mathcal{U}$, and (5) becomes

$$\mathbf{y}_0^{(2)} = \mathbf{D}_0^{(1)}\mathbf{\Pi}_2\psi(\mathbf{\Pi}_1\mathbf{s}) + \mathbf{n}_0^{(2)}. \tag{8}$$

The only difference between (5) and (8) is that the channel matrix $\mathbf{D}_0^{(2)}$ in (5) is replaced by $\mathbf{D}_0^{(1)}$ in (8). From a statistical point of view, the only difference between these two models is the probability distribution of $\mathbf{D}_0^{(1)}$ and $\mathbf{D}_0^{(2)}$; from a practical perspective, we can think of (8) as the limiting case of (5) with perfect decoding in user-to-user links. Regardless of the interpretation, the important points are stated in the following lemmas[1].

[1]Proofs of claims in this paper can be found in [2].

Lemma 1 *If* $\eta(\mathcal{D}) := \lim_{\gamma\to\infty} \log[P_e(\gamma|\mathcal{D})]/\log(\gamma)$ *denotes the diversity order of the MSC protocol* $(\mathbf{\Pi}_2, \psi(\cdot), \mathbf{\Pi}_1)$ *when conditioned on the decoding set* $\mathcal{D}$*, then*

$$\eta(\mathcal{D}) \geq \max[0; \beta - (K - |\mathcal{D}|)], \tag{9}$$

where $|\mathcal{D}|$ *is the cardinality of* $\mathcal{D}$ *and* $\beta := \eta(\mathcal{U})$ *is the diversity order when* $\mathcal{D} \equiv \mathcal{U}$*.*

Lemma 2 *The probability* $\Pr(\mathcal{D})$ *of the decoding set* $\mathcal{D}$ *satisfies*

$$\lim_{\gamma\to\infty} \frac{\log[\Pr(\mathcal{D})]}{\log(\gamma)} = -(K - |\mathcal{D}|). \tag{10}$$

Lemma 1 establishes the intuitively expected result that the diversity order decreases by the number $K - |\mathcal{D}|$ of users who did not decode s correctly. However, Lemma 2 shows that as $\gamma \to \infty$ the probability of this event behaves precisely as $\gamma^{-(K-|\mathcal{D}|)}$. These two effects compensate each other leading to the following.

Theorem 1 *Let* $\eta[\mathbf{\Pi}_2, \psi(\cdot), \mathbf{\Pi}_1]$ *and* $\beta[\mathbf{\Pi}_2, \psi(\cdot), \mathbf{\Pi}_1]$ *be the diversity orders of the MSC protocol and the equivalent single-user protocol with respective input-output relations* (1)-(5) *and* (1)-(8)*. Then, for any encoder* $\psi(\cdot)$ *and permutation matrices* $\mathbf{\Pi}_1$*,* $\mathbf{\Pi}_2$*, it holds that*

$$\eta[\mathbf{\Pi}_2, \psi(\cdot), \mathbf{\Pi}_1] = \beta[\mathbf{\Pi}_2, \psi(\cdot), \mathbf{\Pi}_1]. \tag{11}$$

The value of Theorem 1 is twofold. On the one hand, it establishes that diversity results for SIMO channels carry over to judiciously designed MSC protocols. In particular, two implications of Theorem 1 are stated in the following corollaries.

Corollary 1 *Diversity order of the repetition coding based MSC protocol in* [C1] *is* $\eta(\mathbf{I}, \psi_R(\cdot), \mathbf{I}) = 2$*.*

Corollary 2 *For the MSC protocol based on distributed ECC in* [C2] *with minimum distance* $d_{\min}$ *and code rate* R_c*, there exist matrices* $\mathbf{\Pi}_1(\mathbf{P})$ *and* $\mathbf{\Pi}_2(\mathbf{P})$ *so that*

$$\eta[\mathbf{\Pi}_2(\mathbf{P}), \psi_P(\cdot), \mathbf{\Pi}_1(\mathbf{P})] = \min(d_{\min}, \lfloor 1+K(1-R_c)\rfloor). \tag{12}$$

On the other hand, Theorem 1 establishes that designing good encoders $\psi(\cdot)$ is equivalent to designing diversity-enabling codes for co-located multi-antenna transmitters, motivating the introduction of CFC in a distributed setup.

2.2. Distributed Complex Field Coding

To define a DCFC based MSC protocol, start by specifying the permutation matrices $\mathbf{\Pi}_1$, $\mathbf{\Pi}_2$ as KN-dimensional periodic interleavers. With e_i denoting the i^{th} element of the canonical basis of $\mathbb{C}^{KN}$, we select

$$\begin{aligned}\mathbf{\Pi}_1 = \mathbf{\Pi}_{KN} &:= [\mathrm{e}_1, \mathrm{e}_N, \ldots, \mathrm{e}_{(K-1)N+1}, \mathrm{e}_2, \mathrm{e}_{N+1}, \ldots, \mathrm{e}_{KN}],\\ \mathbf{\Pi}_2 = \mathbf{\Pi}_{NK} &:= [\mathrm{e}_1, \mathrm{e}_K, \ldots, \mathrm{e}_{(N-1)K+1}, \mathrm{e}_2, \mathrm{e}_{K+1}, \ldots, \mathrm{e}_{KN}].\end{aligned} \tag{13}$$

The period of $\mathbf{\Pi}_1 = \mathbf{\Pi}_{KN}$ is K and consequently it changes the ordering of s so that in $\mathbf{r} = \mathbf{\Pi}_1\mathrm{s}$, same symbol indices across users appear consecutively in $\mathbf{r} = [s_{11}, s_{21}\ldots, s_{K1}, s_{12}, \ldots, s_{KN}]^T$. Likewise, the period of $\mathbf{\Pi}_2 = \mathbf{\Pi}_{NK}$ is N, so that $\mathbf{\Pi}_2 = \mathbf{\Pi}_1^T = \mathbf{\Pi}_1^{-1}$.

Now, define the $K \times 1$ vectors $\mathbf{r}_n := [s_{n1}, \ldots, s_{nK}]^T$ and $\mathbf{u}_n := [v_{n1}, \ldots, v_{nK}]^T$, and consider the DCFC based MSC protocol with $\mathbf{u}_n = \mathbf{\Theta}\mathbf{r}_n$ which amounts to setting $\mathbf{\Phi} := \mathrm{diag}(\mathbf{\Theta}, \ldots, \mathbf{\Theta})$ in [C3]. The rationale behind this particular selection is that each block $\{\mathbf{r}_n\}_{n=1}^N$ is coded independently. We finally de-interleave the received blocks at the AP to obtain [c.f. (5)]

$$\mathbf{\Pi}_1\mathbf{y}_0^{(2)} = A(\mathbf{\Pi}_1\mathbf{D}_0^{(2)}\mathbf{\Pi}_2)\,\mathbf{\Phi}\mathbf{r} + \mathbf{\Pi}_1\mathbf{n}_0^{(2)}. \tag{14}$$

Interestingly, since $\mathbf{\Pi}_2 = \mathbf{\Pi}_1^{-1}$ we have $\mathbf{\Pi}_1\mathbf{D}_0^{(2)}\mathbf{\Pi}_2 = \mathrm{diag}(h_1^{(2)}, \ldots, h_K^{(2)}, \ldots, h_1^{(2)}, \ldots, h_K^{(2)})$. Thus, upon defining $\mathbf{y}_{0n}^{(2)} := [y_{n1}^{(2)}, \ldots, y_{nK}^{(2)}]^T$, $\mathbf{n}_{0n}^{(2)} := [n_{n1}^{(2)}, \ldots, n_{nK}^{(2)}]^T$ and $\mathbf{D}_{0n}^{(2)} := \mathrm{diag}(h_1^{(2)}, \ldots, h_K^{(2)})$; and noting that $\mathbf{\Phi}$ is block diagonal, we get

$$\mathbf{y}_{0n}^{(2)} = A\mathbf{D}_{0n}^{(2)}\mathbf{u}_n + \mathbf{n}_{0n}^{(2)} = A\mathbf{D}_{0n}^{(2)}\mathbf{\Theta}\mathbf{r}_n + \mathbf{n}_{0n}^{(2)}; \tag{15}$$

which amounts to separating (14) in N decoupled equations, each involving the $K \times 1$ vectors $\mathbf{r}_n, \mathbf{y}_{0n}^{(2)}, \mathbf{n}_{0n}^{(2)}$ instead of the $KN \times 1$ vectors $\mathbf{r}, \mathbf{y}_0^{(2)}, \mathbf{n}_0^{(2)}$.

If we finally combine $\mathbf{y}_{0n}^{(2)}$ in (15) with its counterpart $\mathbf{y}_{0n}^{(1)} := [y_{n1}^{(1)}, \ldots, y_{nK}^{(1)}]^T$ from (1) corresponding to the channel matrix $\mathbf{D}_{0n}^{(1)} := \mathrm{diag}(h_1 \ldots\ h_K)$, the ML decoder for a DCFC based MSC protocol is given by

$$\hat{\mathbf{r}}_n = \arg\min_{\mathbf{r}_n\in\mathcal{S}^K} \left\| \begin{bmatrix} \mathbf{y}_{0n}^{(1)} \\ \mathbf{y}_{0n}^{(2)} \end{bmatrix}_{2K\times 1} - A \begin{bmatrix} \mathbf{D}_{0n}^{(1)} \\ \mathbf{D}_{0n}^{(2)}\mathbf{\Theta} \end{bmatrix}_{2K\times K} \mathbf{r}_n \right\|. \tag{16}$$

DCFC decoding in (16) operates on $K \times 1$ symbol blocks, reducing complexity considerably relative to a KN-symbol CFC encoder. (Near)-ML decoders, such as the sphere decoder, can be used to obtain $\hat{\mathrm{s}}_n$ from (16) with polynomial average complexity [2]. Moreover, basic CFC results derived for co-located multi-antenna systems [7] can be directly applied to the distributed MSC setup. In particular, it is useful to recall the notion of maximum distance separable (MDS) matrices.

Definition 1 *A matrix* $\mathbf{\Theta}$ *is called MDS with respect to the constellation* $\mathcal{S}$ *if and only if for any two different symbols* $\mathbf{r}_1 \neq \mathbf{r}_2 \in \mathcal{S}$*, all the coordinates of* $\mathbf{\Theta}\mathbf{r}_1$ *and* $\mathbf{\Theta}\mathbf{r}_2$ *are different i.e.,* $[\mathbf{\Theta}\mathbf{r}_1]_i \neq [\mathbf{\Theta}\mathbf{r}_2]_i$*,* $\forall i$*.*

The MDS property assures full-diversity K in SIMO channels [7], a result that leads to the following corollary, establishing the *full-diversity* order of DCFC based MSC.

Corollary 3 *If* $\mathbf{\Theta}$ *is an MDS matrix, the DCFC based MSC protocol in* [C3] *with* $\mathbf{\Phi} = \mathrm{diag}(\mathbf{\Theta}, \ldots \mathbf{\Theta})$ *and* $\mathbf{\Pi}_1$*,* $\mathbf{\Pi}_2$ *given by* (13) *enables diversity equal to the number of users; i.e.,*

$$\eta[\mathbf{\Pi}_2, \mathbf{\Phi}(\cdot), \mathbf{\Pi}_1] = K. \tag{17}$$

3. MULTI-CLUSTER OPERATION

In the multi-cluster setting we have $L > 1$ non-overlapping clusters transmitting to the AP with $\mathbf{s}_{lk} := [s_{lk1}, \ldots, s_{lkN}]^T$ denoting the data packet of U_{lk} and $\mathbf{s}_l := [\mathbf{s}_{l1}^T, \ldots, \mathbf{s}_{lK}^T]^T$ the l^{th} cluster's aggregate block. To separate clusters at the AP we rely on CDMA with S-dimensional spreading codes $\mathbf{c}_l := [c_{l1}, \ldots, c_{lS}]^T$, that we arrange in the matrix $\mathbf{C} = [\mathbf{c}_1, \ldots, \mathbf{c}_L]$. The n^{th} symbol of U_{lk} is transmitted as $\mathbf{x}_{lkn}^{(1)} = A\mathbf{c}_l s_{lkn}$.

The signal $\bar{\mathbf{y}}_{kn}^{(1)}$ received by the AP at time $N(k-1)+n$ is the superposition of the signal transmitted by the L clusters and the AWGN noise, and can be written as

$$\bar{\mathbf{y}}_{kn}^{(1)} = A\sum_{l=1}^{L} h_{lk}\mathbf{c}_l s_{lkn} = A\mathbf{D}_k^{(1)}\mathbf{C}\bar{\mathbf{s}}_{kn} + \mathbf{n}_{kn}^{(1)}, \tag{18}$$

where we defined the vector $\bar{\mathbf{s}}_{kn} := [s_{1kn}, \ldots, s_{Lkn}]^T$ and the channel matrix $\mathbf{D}_k^{(1)} := \mathrm{diag}(h_{k1}, \ldots, h_{kL})$. As usual, we proceed to correlate $\bar{\mathbf{y}}_{kn}$ with each of the signatures in $\mathbf{C}$ so that we transform $\bar{\mathbf{y}}_{kn}^{(1)} \in \mathbb{C}^S$ into the vector $\mathbf{y}_{kn}^{(1)} := \mathbf{C}^{\mathcal{H}}\bar{\mathbf{y}}_{kn}^{(1)} \in \mathbb{C}^L$ leading to the input-output relationship

$$\mathbf{y}_{kn}^{(1)} = A\mathbf{C}^{\mathcal{H}}\mathbf{C}\mathbf{D}_k^{(1)}\bar{\mathbf{s}}_{kn} + \mathbf{n}_{kn}^{(1)} := A\mathbf{R}\mathbf{D}_k^{(1)}\bar{\mathbf{s}}_{kn} + \mathbf{n}_{kn}^{(1)}. \quad (19)$$

Depending on the correlation matrix $\mathbf{R} := \mathbf{C}^{\mathcal{H}}\mathbf{C}$, optimal reception may require *joint* detection of the $L \times 1$ vector $\bar{\mathbf{s}}_{kn}$. While (19) models reception at the AP, a similar relationship characterizes reception in every cooperating user allowing U_{lk} to construct the estimate $\hat{\mathbf{s}}_{lk}$ of its cluster's aggregate block $\mathbf{s}_l$. Similar to Section 2, we define $\mathcal{D}_l := \{U_{lk} \mid \hat{\mathbf{s}}_{lk} = \mathbf{s}_l\} \subseteq \mathcal{U}_l$; and let $h_{lk}^{(2)} = h_{lk}$ if $U_{lk} \in \mathcal{D}_l$, and $h_{lk}^{(2)} = 0$ else. As before, users $U_{lk} \in \mathcal{D}_l$ participate in phase-2.

Each cluster in phase-2 operates separately, processing $\mathbf{s}_l$ as in Section 2.2 to construct $\mathbf{v}_l := [v_{l11}, \ldots, v_{l1N}, v_{l21}, \ldots, v_{lKN}]^T = \mathbf{\Pi}_2\mathbf{\Phi}\mathbf{\Pi}_1\mathbf{s}_l$ with $\mathbf{\Pi}_1$ and $\mathbf{\Pi}_2$ as in (13) and $\mathbf{\Phi} = \mathrm{diag}(\mathbf{\Theta}, \ldots, \mathbf{\Theta}) \in \mathbb{C}^{NK \times NK}$. Each user $U_{lk} \in \mathcal{D}_l$ then transmits the sub-block $\mathbf{v}_{lk} := [v_{lk1}, \ldots, v_{lkN}]^T$ with the n^{th} symbol of U_{lk} in the second phase transmitted as $\mathbf{x}_{lkn}^{(2)} = A\mathbf{c}_l v_{lkn}$. While the encoding steps coincide with those in Section 2.2, the received signal – as in (18) – comprises the superposition of waveforms transmitted from users in all L clusters

$$\bar{\mathbf{y}}_{kn}^{(2)} = A\sum_{l=1}^{L} h_{lk}^{(2)}\mathbf{c}_l v_{lkn} = A\mathbf{D}_{0k}^{(2)}\mathbf{C}\bar{\mathbf{v}}_{kn} + \mathbf{n}_{kn}^{(2)}, \quad (20)$$

where we defined the vector $\bar{\mathbf{v}}_{kn} := [v_{1kn}, \ldots, v_{Lkn}]^T$ and the phase-2 channel matrix $\mathbf{D}_{0k}^{(2)} = \mathrm{diag}(h_{1k}^{(2)}, \ldots, h_{Lk}^{(2)})$. Correlating with the signatures in $\mathbf{C}$ we construct the vector $\mathbf{y}_{kn}^{(2)} := \mathbf{C}^{\mathcal{H}}\bar{\mathbf{y}}_{kn}^{(2)}$ and write $\mathbf{y}_{kn}^{(2)} = A\mathbf{R}\mathbf{D}_{0k}^{(2)}\bar{\mathbf{v}}_{kn} + \mathbf{n}_{kn}^{(2)}$, the counterpart of (19) for phase-2.

Upon defining the vectors $\mathbf{y}_{0n}^{(2)} := [\mathbf{y}^{(2)T}_{1n}, \ldots, \mathbf{y}^{(2)T}_{Kn}]^T$, $\bar{\mathbf{v}}_n := [\bar{\mathbf{v}}_{1n}^T, \ldots, \bar{\mathbf{v}}_{Kn}^T]^T$, the correlation matrix $\bar{\mathbf{R}} := \mathrm{diag}(\mathbf{R}, \ldots, \mathbf{R})$ and the channel $\mathbf{D}_0^{(2)} := \mathrm{diag}(\mathbf{D}_{01}^{(2)}, \ldots, \mathbf{D}_{0K}^{(2)})$ the latter can be written in the more useful form

$$\mathbf{y}_{0n}^{(2)} = A\bar{\mathbf{R}}\mathbf{D}_0^{(2)}\bar{\mathbf{v}}_n + \mathbf{n}_{0n}^{(2)}. \quad (21)$$

Finally, let $\mathbf{u}_{ln} := [u_{l1n}, \ldots, u_{lKn}]^T$, $\mathbf{u}_n := [\mathbf{u}_{1n}^T, \ldots, \mathbf{u}_{Ln}^T]^T$ and $\mathbf{\Pi}_{LK} := [\mathbf{e}_1, \mathbf{e}_L, \ldots, \mathbf{e}_{(L-1)K+1}, \mathbf{e}_2, \mathbf{e}_{K+1}, \ldots, \mathbf{e}_{KL}]$ be a KL-dimensional periodic interleaver with period L. According to these definitions, we have $\bar{\mathbf{v}}_n = \mathbf{\Pi}_{LK}\mathbf{u}_n$. Also, note that since $\mathbf{u}_{ln} = \mathbf{\Theta}\mathbf{r}_{ln}$, for $\mathbf{r}_n := [\mathbf{r}_{1n}^T, \ldots, \mathbf{r}_{Ln}^T]^T$ and $\bar{\mathbf{\Phi}} = \mathrm{diag}(\mathbf{\Theta}, \ldots, \mathbf{\Theta}) \in \mathbb{C}^{LK \times LK}$, we have that

$$\mathbf{y}_{0n}^{(2)} = A\bar{\mathbf{R}}\mathbf{D}_0^{(2)}\mathbf{\Pi}_{LK}\bar{\mathbf{\Phi}}\mathbf{r}_n + \mathbf{n}_{0n}^{(2)}. \quad (22)$$

Concatenating (19) and (22) we obtain the ML decoder

$$\hat{\mathbf{r}}_n = \arg\min_{\mathbf{r}_n \in \mathcal{S}^{LK}} \left\| \begin{bmatrix} \mathbf{y}_{0n}^{(1)} \\ \mathbf{y}_{0n}^{(2)} \end{bmatrix} - A \begin{bmatrix} \bar{\mathbf{R}}\mathbf{D}_0^{(1)} \\ \bar{\mathbf{R}}\mathbf{D}_0^{(2)}\mathbf{\Pi}_{LK}\bar{\mathbf{\Phi}} \end{bmatrix}_{2LK \times LK} \mathbf{r}_n \right\|. \quad (23)$$

Dimensionality of the multi-cluster ML decoder (23) is KL that has to be compared with K, the corresponding dimensionality of the ML decoder in (16) for the single-cluster case.

Even though the input-output relationships (19)-(22) and (1)-(5) model different systems they exhibit similar forms. An important consequence of this observation is that Corollary 3 establishing the diversity order of a single-cluster DCFC based MSC protocol can be readily generalized.

Corollary 4 *If $\mathbf{\Theta}$ is MDS, the multi-cluster DCFC based MSC protocol with the ML decoder in* (23) *achieves diversity equal to the number of users in each cluster; i.e*

$$\eta[\mathbf{\Pi}_2, \bar{\mathbf{\Phi}}, \mathbf{\Pi}_1, \mathbf{R}] = K. \quad (24)$$

As expected, Corollary 4 proves that the diversity enabled by DCFC remains invariant regardless of the structure of the correlation matrix $\mathbf{R}$.

3.1. Effect of under-spreading in spectral efficiency

Transmission of $\mathbf{x}_{lkn}^{(1)}, \mathbf{x}_{lkn}^{(2)}$, requires S times more bandwidth than transmission of s_{lkn}, v_{lkn} and consequently, the spectral efficiency of multi-cluster DCFC is $\xi = L/(2S)$. The spectral efficiency ξ is affected by the selection of $\mathbf{C}$. Indeed, an important factor is whether the spreading gain S *a fortiori* constrains the number of codes L or not, motivating a distinction between *under-spread* and *over-spread* MA:

Definition 2 *In an over-spread MA system, the number of codes L and the spreading gain S are constrained by $L \le S$. We say that an MA system is under-spread if L and S can be selected independently.*

Over-spread orthonormal MA: In this case, $\mathbf{C}$ is formed by orthonormal vectors, e.g., Walsh-Hadamard sequences, so that $\mathbf{R} := \mathbf{C}^{\mathcal{H}}\mathbf{C} = \mathbf{I}_L$. The latter requires $L \le S$ because a set of orthonormal vectors in $\mathbb{C}^S$ cannot contain more than S elements.

Under-spread MA: Symbol-periodic non-orthogonal signatures, including those in MC-CDMA and DS-CDMA with Gold or Kasami sequences [2], implement under-spread MA since L can be much larger than S. Long pseudo-noise (PN) sequences also give rise to under-spread MA. Since L can be theoretically infinite, L and S are clearly decoupled.

MSC protocols with under- and over-spread are fundamentally different in terms of bandwidth efficiency. In over-spread MA the spectral efficiency of MSC protocols is hard limited by $\xi_{\mathrm{MSC}} \le 1/2$ and cooperation comes at the price of reducing the spectral efficiency $\xi_{\mathrm{NC}} = 1$ of the corresponding non-cooperative system. In under-spread MA, ξ and η are not necessarily traded off since L and S are decoupled. Indeed, we can obtain $\xi_{\mathrm{MSC}} = \xi_{NC}$ by reducing the spreading gain by half, i.e., $S_{\mathrm{MSC}} = S_{NC}/2$ while maintaining the same number of clusters L. Note that even if we reduce the spreading gain by half, after completing both MSC phases each information symbol has been transmitted twice and the effective coding gain is still the same as in non-cooperative MA. Nonetheless, a consequence of Corollary 4 is that the diversity gain is $\eta[\mathbf{\Pi}_2, \bar{\mathbf{\Phi}}, \mathbf{\Pi}_1, \mathbf{R}] = K$, regardless of the correlation structure $\mathbf{R}$.

4. COMPARING MSC WITH NON-COOPERATIVE PROTOCOLS

We considered distributed repetition coding (DRC), distributed (D)ECC and DCFC defined in [C1], [C2] and [C3], respectively. We also distinguished between under- and over-spreading for cluster separation as per Definition 2, for a total of six different alternatives. These alternatives differ in diversity η, spectral efficiency ξ and decoding complexity ζ as summarized in Table 1.

Table 1. Comparison of MSC and non-cooperative protocols

spread	metric	DRC	DECC	DCFC	NC
over-	η	2	$\lfloor 1{+}K(1{-}R_c)\rfloor^{(\dagger)}$	K	1
	ξ	1/2	1/2	1/2	1
	ζ	1	KN	K	1
under-	η	2	$\lfloor 1{+}K(1{-}R_c)\rfloor^{(\dagger)}$	K	1
	ξ	1	1	1	1
	ζ	L	LKN	LK	1

$^{(\dagger)}$ Assuming that $d_{\min} > \lfloor 1{+}K(1{-}R_c)\rfloor$. NC = non-cooperative, η = diversity, ξ = spectral efficiency, ζ = decoding complexity.

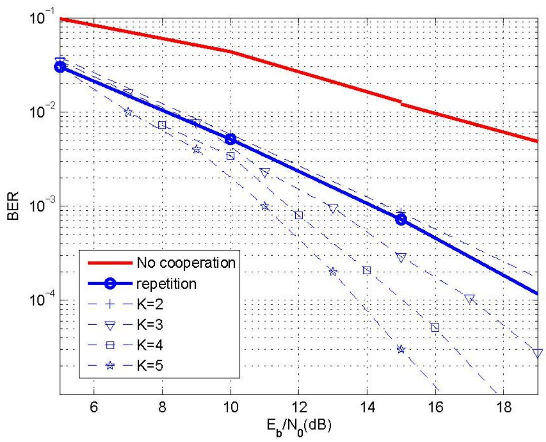

Fig. 3. BER of orthonormal DCFC-based MSC with variable number of users.

DRC affords the lowest decoding complexity, but also enables the smallest diversity order. The diversity order can be increased with either distributed ECC or DCFC at the expense of increasing decoding complexity. Spectral efficiency of over-spread MA, ξ is reduced from 1 to $1/2$ for any of the MSC protocols; whereas, the value of ξ for under-spread MA is not affected when we move from non-cooperative MA to MSC. The value $\xi = 1$ is an arbitrary selection and should be interpreted as an option to allow a fair comparison between over-spread non-cooperative MA and under-spread cooperative MA.

All in all, in a complexity-limited system repetition coding offers the best MSC protocol, while in a bandwidth-limited setup DCFC-based MSC with under-spreading for cluster separation should be preferred. In intermediate cases, DCFC-based MSC with (over-spread) orthonormal cluster separation achieves full diversity with reasonable spectral-efficiency ($\xi = 1/2$) and a modest increase in complexity.

5. SIMULATIONS

For DCFC based MSC the ML decoder operates on blocks of length K, the spectral efficiency is $\xi = 1/2$ and the diversity order is $\eta = K$ (see Table 1). Fig. 3 demonstrates how the bit error rate (BER) varies with K for DCFC based MSC. We verify that the diversity order is, indeed, equal to the number of users K. For reference, we also depict the BER of a non-cooperative system and repetition based MSC [4]. Setting e.g., $K = 5$, we can see that with a minimal investment in decoding complexity, DCFC based MSC returns a $4 - 5$ dB gain with respect to repetition based MSC due to the increase in diversity from $\eta = 2$ to $\eta = K = 5$.

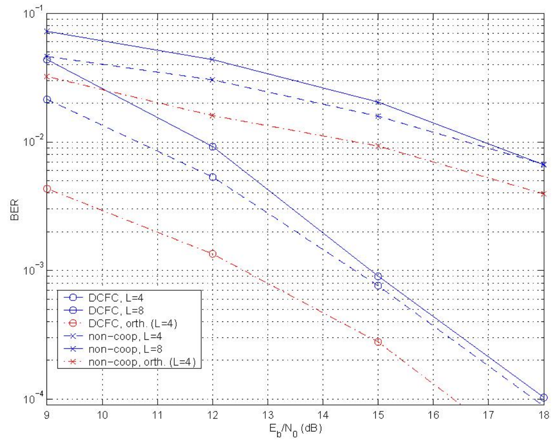

Fig. 4. BER of under-spread DCFC-based MSC with different values of spectral efficiency.

According to Table 1 DCFC with under-spread MA requires ML decoding on blocks of length KL, but attains spectral efficiency $\xi = 1$ and diversity order $\eta = K$. In Fig. 4 we show BER for $K = 3$, $S = 8$ and $L = 4 - L = 8$ with PN codes used to implement under-spread cluster separation. Verifying Corollary 4, the diversity order is $\eta = K = 3$ regardless of the number of clusters L. When $L = 8$ the spectral efficiency is $\xi = 1$ and it is pertinent to compare DCFC with a non-cooperative protocol with orthonormal MA (for which $\xi = 1$ too). The diversity enabled by DCFC leads to a considerable BER reduction. When $L = 4$ the spectral efficiency is $\xi = 1/2$. In this case, it is possible to use DCFC based MSC with orthonormal MA. We can see that gaining in spectral efficiency with DCFC entails a loss in coding gain of about 2dB. Interestingly, the coding gain is affected by the use of under-spread MA but the diversity order is not.

6. REFERENCES

[1] J.Laneman and G.Wornell,"Distributed Space-Time Coded Protocols for Exploiting Coop. Diversity in Wireless Nets.," *IEEE Trans. Inf. Theory*, vol.49, pp.2415-25, Oct. 2003.

[2] A. Ribeiro, R. Wang, and G. Giannakis, "Multi-source coop. with full-diversity spectral-efficiency and controllable-complexity," *IEEE J. Sel. Areas Commun.*, Jan. 2006.

[3] G. Scutari and S. Barbarossa, "Distributed space-time coding for regenerative relay networks," *IEEE Trans. Wireless Commun.*, vol. 4, pp. 2387–2399, Sept. 2005.

[4] A. Sendonaris, E. Erkip, and B. Aazhang, "User coop. diversity," *IEEE Trans. Commun.*, vol.51, pp.1927-48, Nov.2003.

[5] O. Shalvi, "Multiple source cooperation diversity," *IEEE Commun. Letters*, vol. 8, No. 12, pp. 712–714, Dec. 2004.

[6] R. Wang, W. Zhao, and G. B. Giannakis, "Distributed trellis coded modulation for multi-source coop. networks," in *Proc. IEEE Radio Wireless Symp.*, San Diego, CA, Jan., 2006.

[7] Y.Xin, Z.Wang, and G.Giannakis,"Space-time diversity systems based on linear constellation precoding," *IEEE Trans. Wireless Commun.*, vol. 2, no. 2, pp. 294–309, March 2003.